Journal of Power Sources 189 (2009) 726–729

Contents lists available at ScienceDirect

Journal of Power Sources

journal homepage: www.elsevier.com/locate/jpowsour

Short communication

Three-dimensionally ordered macroporous Ni–Sn anode for lithium batteries

Kei Nishikawa [a], Kaoru Dokko [b], Koji Kinoshita [a], Sang-Wook Woo [a], Kiyoshi Kanamura [a,*]

[a] Department of Applied Chemistry, Tokyo Metropolitan University, 1-1 Minami-ohsawa, Hachioji, Tokyo 192-0397, Japan
[b] Department of Chemistry and Biotechnology, Yokohama National University, 79-5 Tokiwadai, Hodogaya-ku, Yokohama 240-8501, Japan

ARTICLE INFO

Article history:
Received 16 June 2008
Received in revised form 24 July 2008
Accepted 15 August 2008
Available online 27 August 2008

Keywords:
Colloidal crystal template
Three-dimensionally ordered macroporous Ni–Sn alloy
Rechargeable lithium batteries

ABSTRACT

A three-dimensionally ordered macroporous (3DOM) Ni–Sn alloy electrode was prepared by electroplating using a colloidal crystal template consisting of monodisperse polystyrene (PS) latex. Scanning electron microscopy observations revealed that the prepared 3DOM Ni–Sn electrode (thickness: 16 μm) had uniform macropores that were 1.0 μm in diameter. The feasibility of using this electrode as the anode in an organic electrolyte for lithium batteries was examined. Although the 3DOM Ni–Sn electrode exhibited a discharge capacity of 455 mAh g^{-1}, the discharge capacity decreased rapidly after 30 charge–discharge cycles owing to the collapse of the porous structure caused by the volume change during lithiation and delithiation.

1. Introduction

Lithium batteries have been widely used as power sources for portable devices because of their high energy density. However, next-generation vehicles such as electric vehicles and plug-in hybrid vehicles require batteries with higher performance than conventional lithium batteries. Carbonaceous materials have been utilized as anode materials for practical lithium batteries. Several researchers have investigated the use of alternative anode materials with an aim to increase the energy density of the lithium battery. Alloy materials, which can react with Li to form Li alloys, are very promising anode materials. One of the most prospective alloys is the Sn-based alloy. However, Sn undergoes considerable volume change during the charge–discharge cycle accompanying the following lithiation reaction:

$$Sn + 4.4Li \leftrightarrow Li_{4.4}Sn \quad (1)$$

This volume change causes disconnection between the active material and the current collector, and eventually leads to collapse of the active material structure. This is the main reason for the poor cyclability of the Sn electrode. In order to overcome the volume change problem, some researchers have focused on the use of Sn-based alloy materials as anodes in lithium batteries. Thackeray et al. reported the electrochemical characteristics and structure change accompanying lithiation for the Sn-based intermetallic electrode by X-ray diffraction (XRD) [1–3]. Sanyo Company reported the feasibility of using electrodeposited thin films of Cu–Sn and Co–Sn alloys [4–6]. Dahn and co-workers carried out systematic researches on Sn-based alloys [7–9]. Furthermore, the Nexelion battery, which has a Sn-based negative electrode (anode), is commercialized by Sony [10].

The Ni–Sn alloy is also a potential candidate for a novel anode material. Ni atoms form a matrix around the Sn atoms; this structure can restrict the volume change of Sn during its electrochemical reaction with Li because the Ni matrix plays only a buffer role, i.e., it does not react with Li. Mukaibo et al. have reported that Ni–Sn thin films prepared by electroplating can deliver a high specific capacity of 600 mAh g^{-1} [11]. However, since the volume change of Sn is not restricted completely, cracks are formed on the electrode surface after repeated charging and discharging.

In this study, the electrode structure is controlled not only on the atomic scale but also on the micron scale. Control of the electrode structure on the atomic scale involves alloying of Sn with Ni, while control on the micron scale involves the fabrication of a three-dimensionally ordered macroporous (3DOM) electrode. Our research group has developed a technique for preparing a 3DOM structure from a suspension of monodisperse spherical particles [12–14]. The advantage of this structure is its regularity and large specific surface area. The macroporous structure is expected to alleviate the volume change of the active material during charging and discharging. We have reported the fabrication of a 3DOM Ni–Sn electrode [15]. Sun and co-workers also reported the fabrication of macroporous electrodes of Sn-based alloys [16–18]. Control of the electrode structure by means of integration between the atomic and submicron levels may be effective in the development of new anode materials for Li-ion batteries.

* Corresponding author. Tel.: +81 42 677 2828; fax: +81 42 677 2828.
E-mail address: kanamura@tmu.ac.jp (K. Kanamura).

0378-7753/$ – see front matter © 2008 Elsevier B.V. All rights reserved.
doi:10.1016/j.jpowsour.2008.08.041

However, the thickness of the macroporous electrode prepared by Sun and co-workers was less than 2 μm [16–18]. The mass of a 2-μm-thick macroporous electrode would be too less for practical use in cylinder-type and laminate batteries. For practical applications, the thickness of the macroporous electrode should be more than 10 μm. Therefore, the construction of a 3DOM Ni–Sn electrode with a thickness more than 10 μm is the objective of this study.

2. Experimental

The 3DOM Ni–Sn alloy was prepared by a combination of the colloidal crystal template method and electroplating. A colloidal crystal consisting of monodispersed polystyrene (PS) spheres was prepared on a Cu substrate by electrophoretic deposition. The monodisperse PS latex (diameter: 1.0 μm) (Interfacial Dynamics Corp.) was used to fabricate the colloidal crystal. The PS spheres were functionalized by amidine groups and had a positive charge. A 0.3-mm-thick Cu plate (Nilaco) was used as the substrate for the electrophoretic deposition, and a Ni plate (Nilaco) was used as the counter electrode. Prior to the electrophoresis experiment, the Cu substrate was polished to a mirror surface. The distance between the Ni electrode and the Cu substrate was 1 cm, and a constant voltage of 20 V was applied between the two electrodes for 15 min. The effective surface area available for electrophoretic deposition was 1.0 cm^2. After electrophoretic deposition, heat treatment (383 K, 10 min) was conducted in order to connect the PS spheres to one another on the substrate. In this manner, a PS template was obtained on the Cu substrate. The porosity of the PS template having a close-packed structure would be 26%.

Before electroplating of the Ni–Sn alloy, the PS template was immersed in ethanol for 30 s in order to improve its wettability, without which the plating solution would not penetrate the PS template. The PS template on the Cu substrate was immersed in the electroplating bath, and the Ni–Sn alloy was deposited on it by electroplating. The bath composition is provided in Table 1. The bath temperature was maintained at 323 K, and the counter electrode used was a Sn plate. A constant current of 1.4 mA was imposed on the Cu substrate using an automatic polarization system (HSV-100, Hokuto Denko Corp.). The thickness of the 3DOM Ni–Sn coating could be easily controlled by adjusting the electroplating time. After electroplating of the Ni–Sn alloy, the electrode was immersed in toluene overnight to remove the PS template. Through this procedure, a Ni–Sn alloy electrode with an inverse-opal structure was obtained. An electrode with an ideal inverse-opal structure would have a porosity of 74%. The morphology of the electrode was observed using a scanning electron microscope (SEM, JSM-5310, JEOL). The crystalline structure of the electrode was characterized by XRD using Cu Kα radiation. The composition of the Ni–Sn alloy was analyzed by X-ray fluorescence spectroscopy (XRF, ZSX 100e, Rigaku).

The electrochemical properties of the 3DOM Ni–Sn electrode were characterized in a beaker-type cell with a two-electrode system. A mixed solvent (ethylene carbonate (EC):diethyl carbonate (DEC) = 1:1) containing 1 mol dm^{-3} $LiClO_4$ was used as the electrolyte, and a 0.3-mm-thick Li foil was used as the counter electrode. Charge–discharge measurements were carried out galvanostatically by using an automatic charge–discharge instrument (HJR-110mSM6, Hokuto Denko Corp.). All the electrochemical measurements were conducted at room temperature in a glove box filled with pure Ar gas.

Table 1
Composition of Ni–Sn electroplating bath

Composition	Concentration (mol dm^{-3})
$NiCl_2 \cdot 6H_2O$	0.075
$SnCl_2 \cdot 2H_2O$	0.175
$K_4P_2O_7$	0.5
Glycine	0.15
NH_4OH (mL L^{-1})	5

3. Results and discussion

Fig. 1(a) shows the SEM image of the PS spheres deposited on the Cu substrate. The deposited spheres had a three-dimensionally ordered structure, and each PS sphere was connected with its nearest neighbors. Fig. 1(b) and (c) shows the SEM images of the 3DOM Ni–Sn electrode obtained after eliminating the PS spheres. The electrodeposited Ni–Sn alloy grew in the space between the stacked PS spheres and assumed an inverse-opal structure, as shown in Fig. 1(b). These SEM images reveal that the macropore size depends on the size of the PS spheres. The thickness of the Ni–Sn electrode was 16 μm, as shown in Fig. 1(c). The mass of the Ni–Sn alloy deposited on the copper substrate was 6.2 mg cm^{-2}. In this study, PS particles that were 1.0 μm in diameter were utilized as the macropore templates. It has been reported that a 0.5-μm-thick Ni–Sn thin film electrode has large specific capacity and long cycle life [11]. By using particles with 1.0 μm diameter as the templates, the wall thickness between macropores in the replicated macroporous structure can be reduced to less than 0.5 μm. As can be seen in Fig. 1(b), the maximum wall thickness between the macropores is 0.45 μm. Fig. 2 demonstrates the XRD pattern of the prepared Ni–Sn 3DOM electrode. The XRD peaks were attributed to Ni_3Sn_4 and the Cu substrate, and it was confirmed that Ni_3Sn_4 is the predominant phase in the deposited film. XRF analysis revealed that the atomic ratio of Ni/Sn in the 3DOM Ni–Sn alloy was 40/60. This alloy composition slightly deviated from the ideal composition expected for Ni_3Sn_4. This might be due to the existence of a small amount of the Ni_xSn_y metastable phase [19], although it was not detected by XRD.

Fig. 3 shows the charge–discharge curves of the 3DOM Ni–Sn electrode measured at a current density of 50 mA g^{-1}. During charging, lithiation of the Ni–Sn alloy takes place at a potential lower than 0.5 V, while during discharging, delithiation occurs at around 0.5 V. It is considered that the electrochemical reaction of Ni–Sn occurs, involving the formation of the $Li_{4.4}Sn$ alloy and the separation of Ni [20]:

$$Ni_3Sn_4 + 17.6Li^+ + 17.6e^- \rightarrow 4Li_{4.4}Sn + 3Ni \quad (2)$$

During the lithiation process, the crystallographic structure of Li_xSn changes with the value of x. Mukaibo et al. have reported that the Ni_3Sn_4 phase is reformed during discharging (delithiation) [21]. In any case, several phase transitions take place during the charge–discharge cycle. The charging and discharging capacities of the 3DOM Ni–Sn alloy in the first cycle were 392 and 324 mAh g^{-1}, respectively. The theoretical capacity of the Ni–Sn (60 at.% Sn) alloy is calculated to be 747 mAh g^{-1} on the basis of the assumption that 4.4Li react with one Sn atom in the Ni–Sn alloy. Mukaibo et al. [11] and Scrosati and co-workers [19] reported that Ni–Sn thin films prepared by electroplating exhibited discharge capacities higher than 500 mAh g^{-1}. Although the charge–discharge test in this study was carried out at a very low current density of 50 mA g^{-1}, the specific discharge capacity of 3DOM Ni–Sn was smaller than that of the thin-film electrodes [11]. As mentioned later in the document, the volume change of the Ni–Sn alloy due to lithiation and delithiation cannot be completely alleviated by the 3DOM structure. The molar volume of $Li_{4.4}Sn$ is four times larger than that of pure Sn [22].

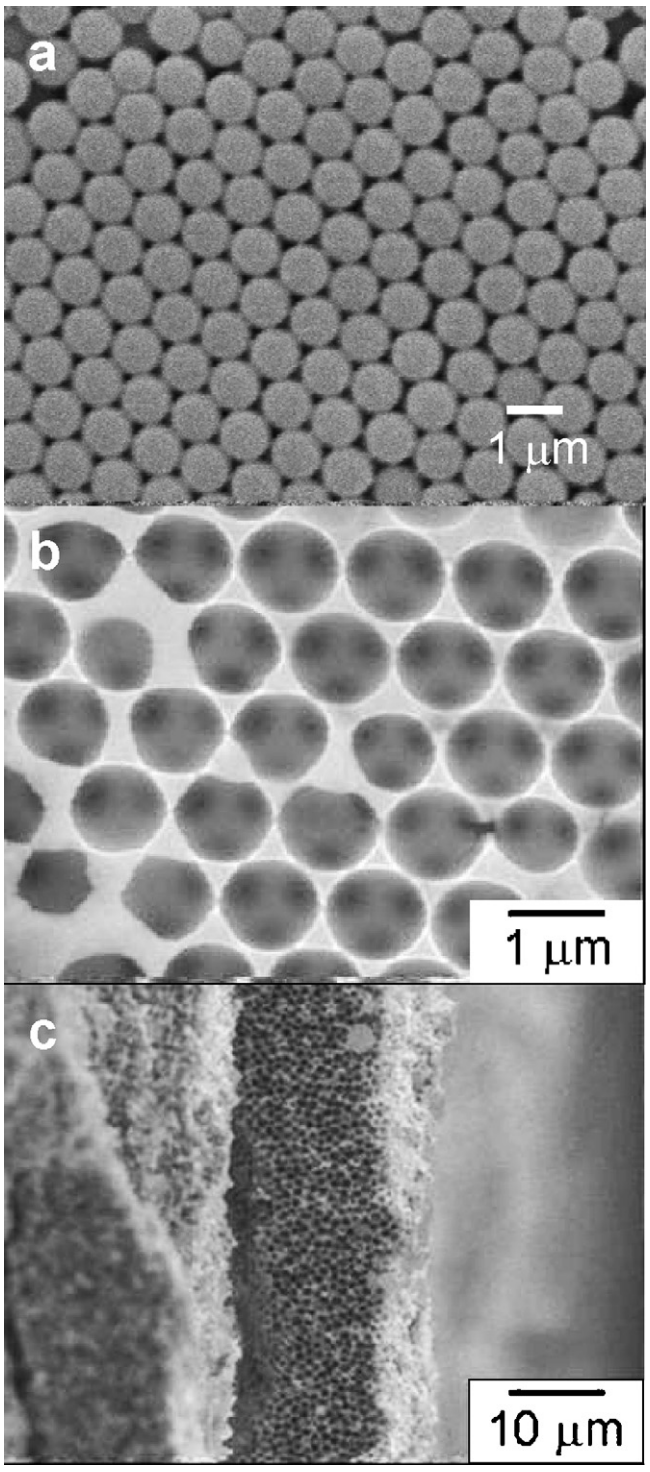

Fig. 1. SEM images of the PS spheres (a), surface of 3DOM Ni–Sn (b), and cross-section of the electrode (c).

The volume expansion during charging might cause shutdown of the connecting windows between the macropores [23], and thus, would isolate the active material from the electrolyte and hinder the electrochemical lithiation reaction inside the porous electrode. Probably, this shutdown led to a decrease in the utilization of the active material.

Fig. 4 shows the dependence of the discharge capacity of the 3DOM Ni–Sn electrode on the number of charge–discharge cycles.

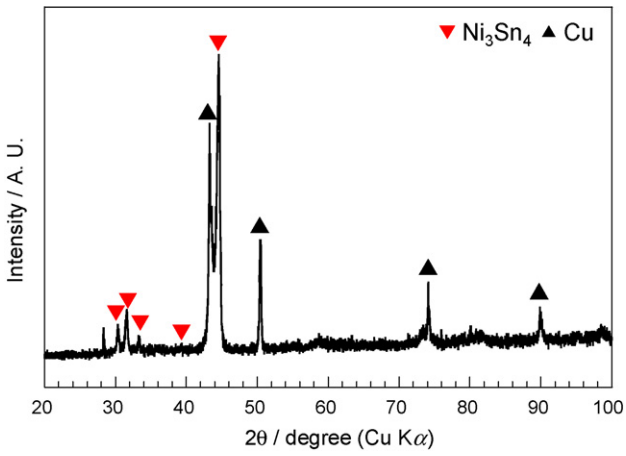

Fig. 2. XRD pattern of 3DOM Ni–Sn electrode prepared on Cu substrate.

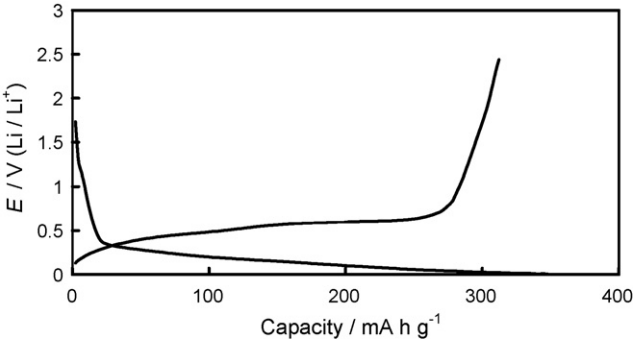

Fig. 3. Initial charge–discharge curves of 3DOM Ni–Sn electrode measured at a current density of 50 mA g^{-1}.

The discharge capacity increased up to the first 30 charge–discharge cycles and then decreased rapidly. Fig. 5(a) displays the SEM image of the 3DOM Ni–Sn electrode after the first charge–discharge cycle. The cracks formed on the electrode surface by the volume change of Sn at the beginning of charge–discharge cycle test probably made fresh Ni–Sn sections on the electrode electrochemically active. Probably, this activation process increased the discharge capacity of the electrode up to 30 cycles, with the capacity reaching a maximum of 455 mAh g^{-1}. Such a cracking phenomenon has also been observed in thin-film Sn-based alloy electrodes, as reported by

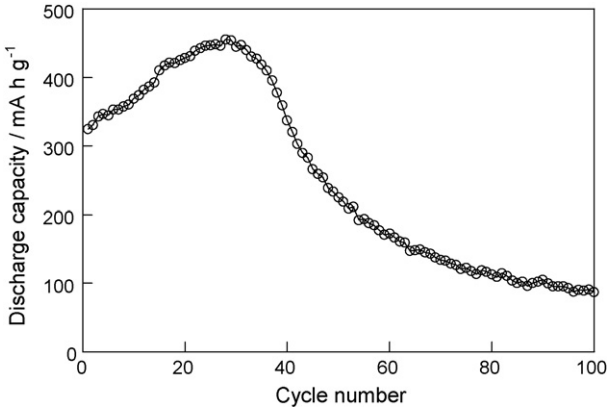

Fig. 4. Dependence of discharge capacity of 3DOM Ni–Sn electrode on number of charge–discharge cycles. Charge–discharge cycle test was carried out at a current density of 50 mA g^{-1}.

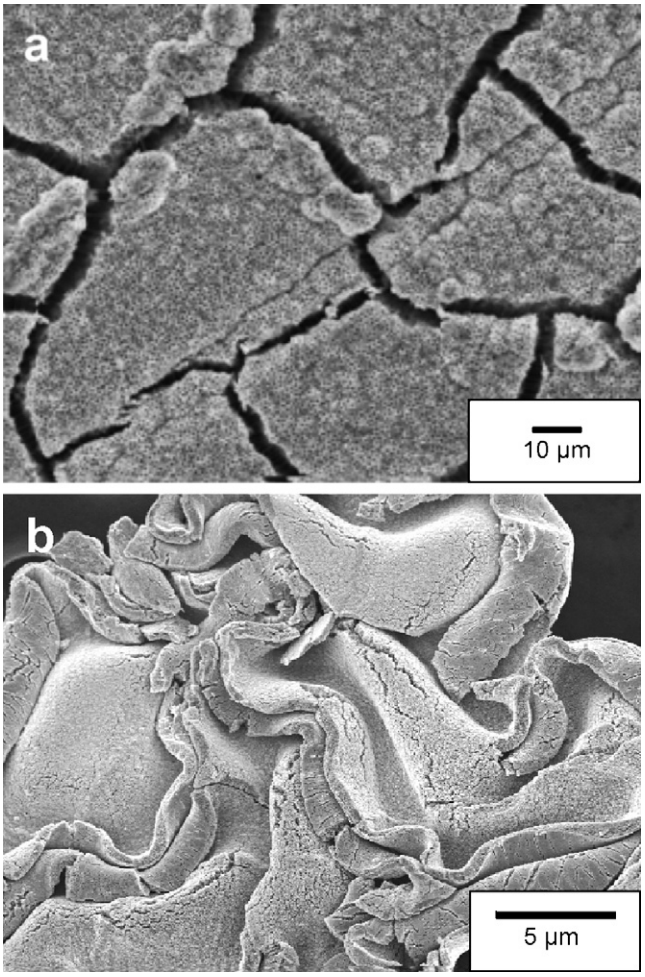

Fig. 5. SEM images of 3DOM Ni–Sn electrodes after the first cycle (a) and after 100 cycles (b).

several groups [5,21,22]. However, further charge–discharge cycles caused delamination of the 3DOM Ni–Sn from the current collector. Fig. 5(b) shows the structure of the 3DOM Ni–Sn electrode after 100 charge–discharge cycles. The 3DOM Ni–Sn film was completely delaminated from the current collector. This brings about a rapid decrease in the electrode capacity owing to the destruction of the electronic conduction path. Delamination of the active material can prove to be fatal for the cycle life and safety of a Li-ion battery. Therefore, sizes of the macropores and the connecting windows and wall thickness between the macropores should be further optimized in order to use the 3DOM Ni–Sn alloy as the anode material in lithium batteries.

4. Conclusion

A 16-μm-thick 3DOM Ni–Sn alloy electrode was prepared on a Cu substrate by the colloidal crystal templating method. The feasibility of the using the 3DOM electrode with a pore diameter of 1.0 μm as the anode in lithium batteries was studied. The 3DOM Ni–Sn electrode exhibited a discharge capacity of 455 mAh g^{-1}. The volume change of Ni–Sn during lithiation and delithiation resulted in the formation of cracks, which in turn brought about a rapid decrease in the discharge capacity. Optimization of the porous structure for improving the discharge capacity and cyclability of the 3DOM Ni–Sn electrode is underway.

Acknowledgement

This work was partially supported by “Development of High-performance Battery System for Next-generation Vehicles Project” from the New Energy and Industrial Technology Development Organization (NEDO) of Japan.

References

[1] M.M. Thackeray, J.T. Vaughey, C.S. Johnson, A.J. Kropf, R. Benedek, L.M.L. Fransson, K. Edstrom, J. Power Sources 113 (2003) 124.
[2] K.D. Kepler, J.T. Vaughhey, M.M. Thackeray, Electrochem. Solid-State Lett. 2 (1999) 307.
[3] L. Fransson, E. Nordstrom, K. Edstrom, L. Haggstrom, J.T. Vaughey, M.M. Thackeray, J. Electrochem. Soc. 149 (2002) A736.
[4] N. Tamura, R. Ohshita, M. Fujimoto, S. Fujitani, M. Kamino, I. Yonezu, J. Power Sources 107 (2002) 48.
[5] N. Tamura, Y. Kato, A. Mikami, M. Kamino, S. Matsuta, S. Fujitani, J. Electrochem. Soc. 153 (2006) A1626.
[6] N. Tamura, Y. Kato, A. Mikami, M. Kamino, S. Matsuta, S. Fujitani, J. Electrochem. Soc. 153 (2006) A2227.
[7] S.D. Beattie, J.R. Dahn, J. Electrochem. Soc. 152 (2005) C549.
[8] A. Timmons, J.R. Dahn, J. Electrochem. Soc. 153 (2006) A1206.
[9] A.D.W. Todd, R.E. Mar, J.R. Dahn, J. Electrochem. Soc. 154 (2007) A597.
[10] H. Inoue, Paper no. 228 Presented at the International Meeting on Lithium Batteries, Biarritz, France, June 18–23, 2006.
[11] H. Mukaibo, T. Sumi, T. Yokoshima, T. Momma, T. Osaka, Electrochem. Solid-State Lett. 6 (2003) A218.
[12] K. Dokko, N. Akutagawa, Y. Isshiki, K. Hoshina, K. Kanamura, Solid State Ionics 176 (2005) 2345.
[13] S.W. Woo, K. Dokko, K. Kanamura, Electrochim. Acta 53 (2007) 79.
[14] H. Munakata, S. Ochiai, K. Kanamura, J. Electrochem. Soc. 154 (2007) B871.
[15] K. Kanamura, A. Ban, K. Dokko, Battery Technology (Denchi Gijyutsu) 17 (2005) 98.
[16] F.S. Ke, L. Huang, J.S. Cai, S.G. Sun, Electrochim. Acta 52 (2007) 6741.
[17] F.S. Ke, L. Huang, H.B. Wei, J.S. Cai, X.Y. Fan, F.Z. Yang, S.G. Sun, J. Power Sources 170 (2007) 450.
[18] F. Ke, L. Huang, H.H. Jiang, H.B. Wei, F.Z. Yang, S.G. Sun, Electrochem. Commun. 9 (2007) 228.
[19] J. Hassoun, S. Panero, B. Scrosati, J. Power Sources 160 (2006) 1336.
[20] I. Amadeia, S. Panero, B. Scrosati, G. Cocco, L. Schiffini, J. Power Sources 143 (2005) 227.
[21] H. Mukaibo, T. Momma, M. Mohamedi, T. Osaka, J. Electrochem. Soc. 152 (2005) A560.
[22] M. Winter, J.O. Besenhard, Electrochim. Acta 45 (1999) 31.
[23] J.C. Lytle, H. Yan, N.S. Ergang, W.H. Smyrl, A. Stein, J. Mater. Chem. 14 (2004) 1616.